Journal of Alloys and Compounds 713 (2017) 64–68

Contents lists available at ScienceDirect

Journal of Alloys and Compounds

journal homepage: http://www.elsevier.com/locate/jalcom

The transparent all-solid-state rechargeable micro-battery manufacturing by RF magnetron sputtering

Suat Pat [a, *], Soner Özen [a], H. Hakan Yudar [a], Şadan Korkmaz [a], Zerrin Pat [b]

[a] Eskişehir Osmangazi University, Physics Department, 26480, Eskişehir, Turkey
[b] Bilecik Şeyh Edebali University, Chemistry Department, Bilecik Turkey

ARTICLE INFO

Article history:
Received 10 March 2017
Received in revised form
2 April 2017
Accepted 14 April 2017
Available online 17 April 2017

Keywords:
Solid-state battery
Transparent battery
Impedance analysis
Equivalent circuit

ABSTRACT

In this paper, a transparent all-solid-state battery was manufactured by RF magnetron sputter, for the first time. $LiFePO_4$ and $Li_4Ti_5O_{12}$ are popular cathode and anode materials, respectively. For the solid-state electrolyte coating, the Li_3PO_4 material is also promising solid electrolyte materials due to the high ionic conductivity. The stack structure of the battery was *silver paste/anode* ($Li_4Ti_5O_{12}$)*/electrolyte* (Li_3PO_4)*/cathode* ($LiFePO_4$)*/ITO/glass*. An indium tin oxide (ITO) coated glass substrate was used as a transparent and conductive material. The resistance of the coated ITO layer is 40 Ω. RF power for the $LiFePO_4$, Li_3PO_4, and $Li_4Ti_5O_{12}$ layers deposition process was adjusted to 100 Watt at argon atmosphere. This stack structure didn't contain any liquid or gel electrolyte layer. The fully solid electrolyte was deposited by the RF magnetron sputter. The mean crystallite sizes of the deposited layers approximately 30 nm, 21 nm and 30 nm for $LiFePO_4$, Li_3PO_4 and $Li_4Ti_5O_{12}$ layer, respectively. The transparency of the manufactured battery is approximately 80%. Electrochemical impedance analyses and cyclic voltammetry measurements were done. The Nyquist diagram and equivalent circuit model were determined. Warburg constant and Li-ion diffusion coefficient were calculated approximately 38 $\Omega/s^{-1/2}$ and 4.2 $\times$ 10^{-10} cm^2/s, respectively. The capacity of the transparent all-solid-state battery was measured as to be 600 μAh/g. The value of the According to obtained results, deposited battery is a quasi-reversible system because of the differences between cathodic and anodic peak potential is calculated about 52 mV. Warburg, Li-ion diffusion coefficient and capacity of the deposited battery show very good adherence with literature.

1. Introduction

Rechargeable or secondary type batteries are very popular for the energy storage system. These batteries are used in electronic devices such as an electrical vehicle (EVs), smartphone, laptops, rechargeable mobile communication tools, microelectronics, medical components, etc. Lithium batteries are the most popular among the rechargeable batteries [1]. Variously physical and chemical deposition methods have been used for fully solid state or thin film battery. These battery types do not contain any liquid or gel electrolytes. But, their sizes are very small according to commercial battery types. Transparent batteries are the key component for the fully transparent electronic devices such as touch screen, display, solar cell, smart watch and phones and etc.

$LiCoO_2$ [1–6], $LiMn_2O_4$ [4], $LiFePO_4$ [7] compounds have been used as cathode materials for the all-solid-state batteries. Lithium phosphorous oxy-nitride (LiPON) electrolyte has high ionic conductivity and chemical stability according to metallic Li [8]. Deposited LiPON layer is a fully solid state electrolyte. An alternative electrolyte is Li_3PO_4 [9], because the Li_3PO_4 material is also promising solid electrolyte materials due to the higher ionic conductivity [10]. Variously intermetallic, ceramic and compounds were investigated as to be battery materials [1–18].

In this research, a highly transparent fully solid-state battery was manufactured by RF sputter deposition method, for the first time. The manufactured transparent rechargeable battery contains transparent conductive layer as cathode current collector, cathode, fully solid-state electrolyte, an anode, and anode current collector. As a substrate material, glass substrates were used for the manufacturing. Firstly, indium thin oxide layer coated on glass substrates by RF magnetron sputtering. Then, $LiFePO_4$ cathode layer was coated on the ITO/glass samples. For the reach final stack of the battery, Li_3PO_4 solid electrolyte, and $Li_4Ti_5O_{12}$ anode layer were coated, respectively. Finally, the silver paste was used for the anode

* Corresponding author.
E-mail address: suatpat@ogu.edu.tr (S. Pat).

http://dx.doi.org/10.1016/j.jallcom.2017.04.169
0925-8388/

current collector. Final sack was formed as to be *silver paste/anode/electrolyte/cathode/ITO/glass.* The transmittances and absorbance of the deposited layer were determined using a UV–Vis spectrophotometer. Field emission scanning electron microscopy (FESEM) was used for the surface morphology characterizations. X-ray diffraction analyses were done for the deposited layers. A Potentiostat was used for the electrochemical impedance analysis and cyclic voltammetry. The capacity of the manufactured battery was determined. Also, electrochemical equivalent circuit and value of the circuit elements were determined by ZSim software.

2. Experimental details

Transparent solid-state rechargeable batteries have been produced using RF magnetron sputter at argon atmosphere. Transparent battery stack was generated as to be *silver paste/anode/electrolyte/cathode/ITO/glass.* Before the coating process, glass substrates were cleaned by deionized water and ethyl alcohol. The 2 inches sputtering target were used for the all deposition process. The transparent conductive layer was deposited from an indium tin oxide (ITO) target. The deposition process was realized at 6.10^{-2} Torr at argon atmosphere. Measurement resistance values of the coated layers per a cm were 40 Ω. Lithium iron phosphate ($LiFePO_4$) cathode materials, lithium phosphate (Li_3PO_4) and lithium titanate ($Li_4Ti_5O_{12}$) anode materials were deposited at 100 W RF power at argon atmosphere. Deposition pressure was adjusted to 2.10^{-1} Torr. All experiments were realized only an hour. RF magnetron sputtering process parameters are summarized in Table 1. Distances of the substrate from the target were kept constant and its value was 50 mm. Throughout the whole depositions process, all parameters kept constant.

3. Experimental results

The surface images of the deposited cathode ($LiFePO_4$), a solid electrolyte (Li_3PO_4) and anode ($Li_4Ti_5O_{12}$) layers were taken using field emission scanning electron microscopy (FESEM). ZEISS Supra 40VP FESEM was used for the surface imaging. The FESEM images of the cathode, solid electrolyte and anode layers are shown in Fig. 1(a) and (b) and 1(c), respectively. These images were obtained at 150,000× magnification. As can be seen in Fig. 1(a)–(c) deposited surface are in uniform, homogeny, compact and nano-structured. Granular structures are clearly seen in FESEM images.

A Panalytical Empriyan XRD tool was used for the estimation XRD pattern, average particle size and phase analysis of the deposited layers. The XRD patterns are shown in Fig. 2(a), b and c. The XRD patterns illustrated in Fig. 2(a), b and 2c belong to $LiFePO_4$, Li_3PO_4 and $Li_4Ti_5O_{12}$ layer. The estimated reflection planes were assigned in the XRD patterns. The determined peak positions for $LiFePO_4$ layer are 42.85° and 44.53°, correspond to (112) and (321) plane. It is indicates that $LiFePO_4$ exist in polycrystalline form. In Fig. 2(b), the XRD peaks, located at 41.91° and 47.26° were indexed as (202) and (301) for the Li_3PO_4 layer. Then, the peaks for $Li_4Ti_5O_{12}$ layer was indexed as to be (400) and (331) located at 44.53° and 47.26°, respectively. The crystallite orientation and surface structure of the deposited layers directly play an important role the Li-ion diffusion capacity [16,22]. These are the key parameters for the battery performance. The layers contains nano particles improve the rate capacities.

Debye-Scherrer equation is the basic equation to determine the mean crystallite size of the deposited layers. XRD peak shape gives more information about the crystallite structures of the deposited layers. The equation can be written as;

$$\textit{mean size of the crystalline} = \frac{K\,\lambda}{\beta * Cos\theta} \quad (1)$$

where, K is a dimensionless shape factor (0.9), λ is the used x-ray wavelength for the analysis and β is the line broadening at half the maximum intensity (FWHM). The calculated mean crystallite sizes are approximately 30 nm, 21 nm and 30 nm for $LiFePO_4$, Li_3PO_4 and $Li_4Ti_5O_{12}$ layer, respectively. These obtained results from the XRD patterns were in rapport with FESEM images. Also, lattice strain value of the deposited layers was determined as to be 0.0033, 0.0047 and 0.0032, respectively.

Unico UV–Vis 4802 double beam spectrophotometer was used for the transmittance and absorbance spectra of the full stack of the battery. Measurements were done in the range of 300–1000 nm. Full stack structure was *silver paste/anode/electrolyte/cathode/ITO/glass.* Transmittance and absorbance spectra of the battery are illustrated in Fig. 3(a) and (b). As can be seen from transmittance graph, the obtained layer is transparent. Transparency values of the *anode/electrolyte/cathode/ITO/glass* are approximately 80% in the visible region. In Fig. 3(a), a photo image of the manufactured battery is seen. Non-coated glass transmittance value is approximately 90% in the visible region. Absorption values of the full stack are also very low.

The reflectance spectrum of the battery stack structure (*anode/electrolyte/cathode/ITO/glass*) was recorded using by Filmetrics F20 interferometer. The reflectance measurement was realized in the range of the 400–1000 nm. An obtained reflectance spectrum is shown in Fig. 4. As can be seen in Fig. 3, battery surface has a colour.

A Gamry potentiostats/galvanostat Reference 3000 was used for the electrochemical measurements. The electrochemical impedance analyses (EIS), cyclic voltammetry (CV) analyses, charge test and capacity measurements were done. Generally, the performance value of the all-solid-state battery is related with the microstructural and surface properties of the layers [22–28]. A Nyquist diagram, an equivalent circuit of the battery and equivalent circuit elements values were obtained from the ZSim software by a fitting procedure. The Nyquist diagram and equivalent circuit diagram were shown in Fig. 5. Impedance spectra were done in an air atmosphere and room temperature with two-probe technique. ZSim software was used to determine equivalent circuit and circuit elements. Obtained circuit elements values were listed in Table 2. A Warburg impedance is related with the Li-ion transfer. Warburg impedance is detected at low frequency region. The straight line at 45° in Fig. 5 is related with the Warburg impedance. Warburg impedance value was obtained approximately 38 $\Omega/s^{-1/2}$.

The cyclic voltammetry (CV) graphs of the fully transparent solid-state battery are seen in Fig. 6. Fig. 6 shows an example of the typical redox curves. The CV measurement was performed at room temperature with the scan rate of 1 mV/s. The CV analyses were applied the deposited all-solid-state battery at atmospheric pressure and room temperature. Li^+ diffusion can calculate using the CV analyses. Li^+ diffusion rate is related with the crystalline structure of the deposited layers. All deposited layers are in the polycrystalline form, according to XRD data shown in Fig. 2. The area of the staked all-solid-state battery was approximately 1 cm^2. The CV scan is shown in the range of 3.80–3.85 V in Fig. 6. These results of the manufactured battery are very similar to related literature. The

Table 1
RF magnetron sputtering parameters.

Parameters, symbol, unit	$LiFePO_4$	Li_3PO_4	$Li_4Ti_5O_{12}$
Pressure, P (Torr)	2×10^{-1}	2×10^{-1}	2×10^{-1}
Buffer gas	Ar of 100%	Ar of 100%	Ar of 100%
RF power, P (Watt)	100	100	100
Time, t (mins)	60	60	60

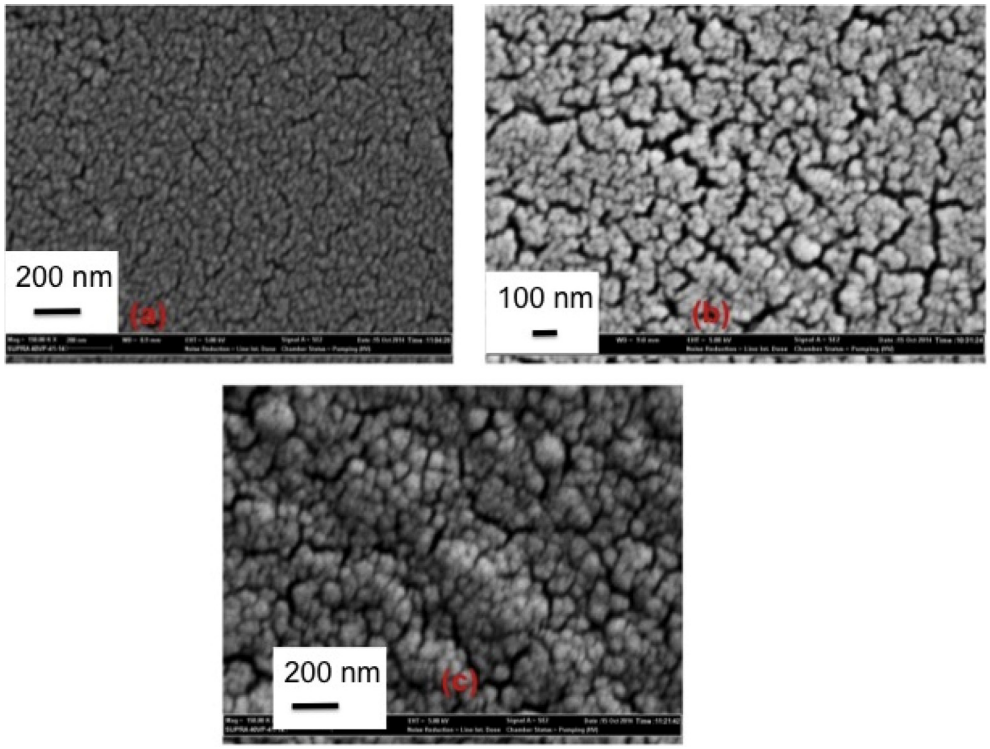

Fig. 1. FESEM images of the nano-layered deposited (a) $LiFePO_4$, (b) Li_3PO_4 and (c) $Li_4Ti_5O_{12}$ layer.

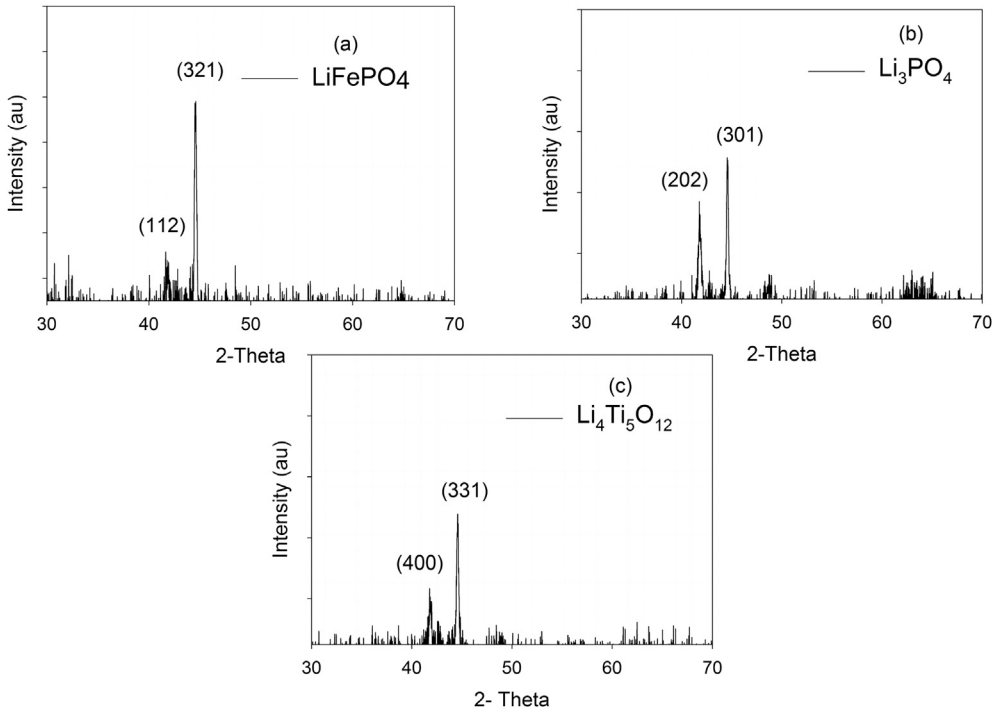

Fig. 2. XRD pattern of the nano-layered deposited (a) $LiFePO_4$, (b) Li_3PO_4 and (c) $Li_4Ti_5O_{12}$ layer.

anodic and cathodic peaks were observed. For the scan rate of 1 mV/s, anodic and cathodic peak values were shifted to 3.86 V and 3.808 V, respectively. The differences between the cathodic and anodic peak potential is calculated about 52 mV. This value is lower than the expected value in the reversible systems potential requirement (59 mV). The obtained this value shows that manufactured battery is a quasi-reversible system [27]. This result is in good harmony with the related literature. The anodic peak positions shift to higher value with increasing scan rate [18,26,27].

By using CV data, the Li^+ ion diffusion coefficient can be

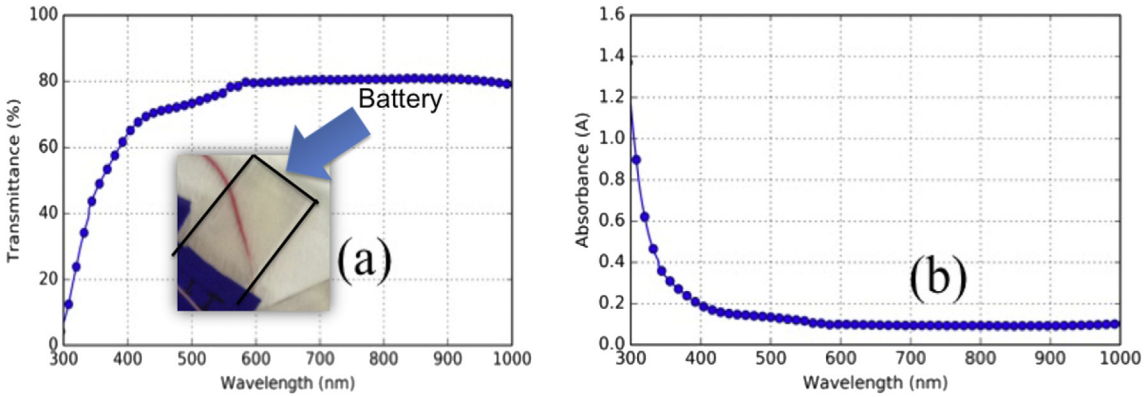

Fig. 3. (a) Transmittance and (b) absorbance spectra of the manufactured battery.

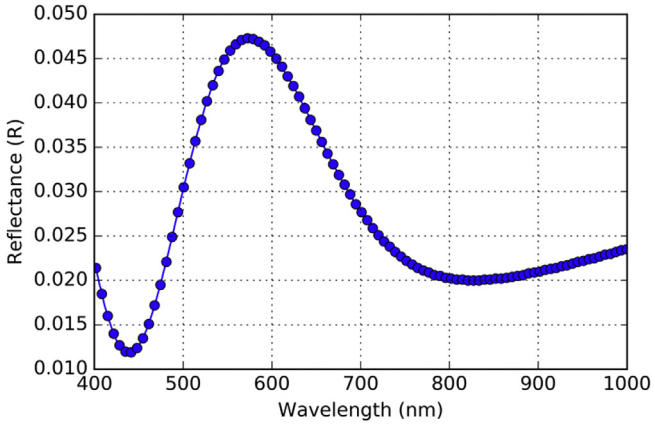

Fig. 4. Reflectance spectra of the full stack battery.

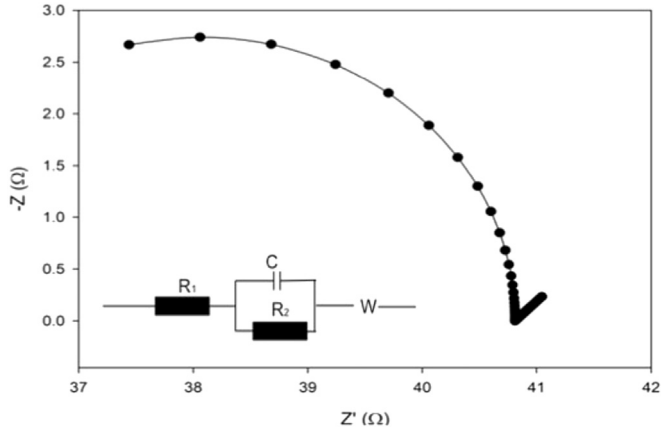

Fig. 5. The Nyquist diagram and equivalent circuit diagram of the battery.

Table 2
Equivalent circuit elements values.

Symbol, Unit	Value
R_1 (Ω)	35
C (nF)	40
R_2 (Ω)	5.5
W, (Ω/$s^{-1/2}$)	38
Chi square	1.3×10^{-5}

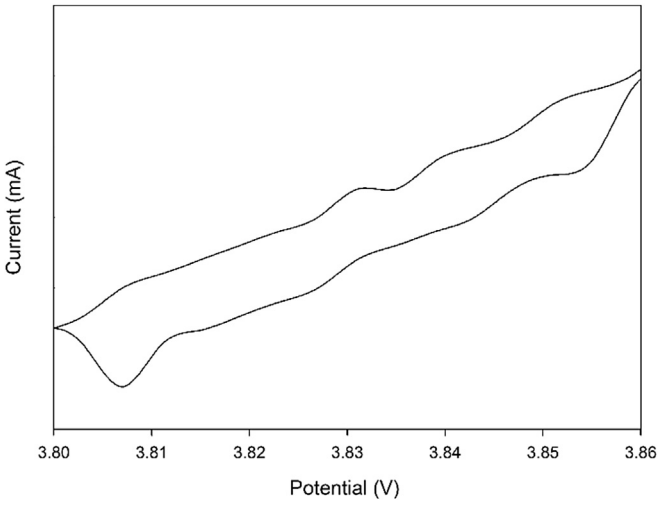

Fig. 6. The CV graph of the transparent solid-state battery.

calculated from the following equation;

$$I_p = 2.6x10^5 n^{3/2} A D_{Li}^{1/2} C_{Li}^{*} \nu^{1/2} \quad (2)$$

where n is the ionization number, A is the area of the electrode, D_{Li} is the Li^+ diffusion coefficient (cm^2/s), C_{Li}^{*} is the bulk concentration of Li-ion in the Li_3PO_4 solid thin film electrolyte (mol/cm^3), and ν is the scan rate of the CV analyses (1 mV/s) [16]. Li^+ ion diffusion value was calculated approximately 4.2×10^{-10} cm^2/s. This value is very good adherence with the literature [13–19]. The capacity of the manufactured battery was calculated as to be 600 μAh/g. This capacity value is very close to commercial product. The properties of the product were introduced by Larfaillou et al., 2016 [20,21].

4. Conclusion

In this research paper, a fully transparent all-solid-state rechargeable battery was manufactured, for the first time. The manufacturing method was RF magnetron sputtering system at argon atmosphere. The stack structure was *silver paste/anode/electrolyte/cathode/ITO/glass.* Field emission scanning electron microscopy images and X-ray diffraction patterns of the all deposited layers were obtained. All deposited layers are in polycrystalline structure. Crystalline structure and surface morphology affects the battery performance. The mean crystallites sizes of the layers are

approximately 30 nm, 21 nm and 30 nm for $LiFePO_4$, Li_3PO_4 and $Li_4Ti_5O_{12}$ layer, respectively. The coated surfaces are homogeny and uniform. According to optical results, the film transparency is very high, approximately 80%. Also, electrochemical analyses including electrochemical impedance spectroscopy, current-voltage analyses, capacity equivalent circuit model, and parameters were determined. Furthermore, Li-ion diffusion coefficient for the transparent all-solid-state battery was calculated as to be approximately 4.2×10^{-10} cm^2/s. Warburg constant value for the fully transparent battery was obtained approximately 38 $\Omega/s^{-1/2}$. The obtained this value shows that manufactured battery is a quasi-reversible system. The differences between the cathodic and anodic peak potential is calculated about 52 mV. All obtained electrochemical results show very good adherence. These results show that fully transparent all-solid-state rechargeable battery manufacturing is possible for the mobile devices.

Acknowledgement

This work fully supported by Tübitak (Grant number is 115E331).

References

[1] J.P. Carmo, R.P. Rocha, A.F. Silva, L.M. Goncalves, J.H. Correia, A thin-film rechargeable battery for integration in stand-alone microsystems, Procedia Chem. 1 (1) (2009) 453–456.
[2] D. Li, Z. Ma, J. Xu, Y. Li, K. Xie, High temperature property of all-solid-state thin film lithium battery using LiPON electrolyte, Mater. Lett. 134 (2014) 237–239.
[3] S. Shiraki, H. Oki, Y. Takagi, T. Suzuki, A. Kumatani, R. Shimizu, T. Hitosugi, Fabrication of all-solid-state battery using epitaxial LiCoO 2 thin films, J. Power Sources 267 (2014) 881–887.
[4] J.B. Bates, N.J. Dudney, B. Neudecker, A. Ueda, C.D. Evans, Thin-film lithium and lithium-ion batteries, Solid State Ionics 135 (1) (2000) 33–45.
[5] N.J. Dudney, Y.I. Jang, Analysis of thin-film lithium batteries with cathodes of 50 nm to 4 μm thick LiCoO 2, J. Power Sources 119 (2003) 300–304.
[6] Y.N. Zhou, M.Z. Xue, Z.W. Fu, Nanostructured thin film electrodes for lithium storage and all-solid-state thin-film lithium batteries, J. Power Sources 234 (2013) 310–332.
[7] M. Köhler, F. Berkemeier, T. Gallasch, G. Schmitz, Lithium diffusion in sputter-deposited lithium iron phosphate thin-films, J. Power Sources 236 (2013) 61–67.
[8] S. Nowak, F. Berkemeier, G. Schmitz, Ultra-thin LiPON films–Fundamental properties and application in solid-state thin film model batteries, J. Power Sources 275 (2015) 144–150.
[9] Y. Kobayashi, H. Miyashiro, K. Takei, H. Shigemura, M. Tabuchi, H. Kageyama, T. Iwahori, 5 V class all-solid-state composite lithium battery with Li3 PO 4 coated LiNi0. 5Mn1. 5 O 4, J. Electrochem. Soc. 150 (12) (2003) A1577–A1582.
[10] N.I. Ayu, E. Kartini, L.D. Prayogi, M. Faisal, Crystal structure analysis of Li3PO4 powder prepared by wet chemical reaction and solid-state reaction by using X-ray diffraction (XRD), Ionics 22 (7) (2016) 1051–1057.
[11] R. Kohler, P. Smyrek, S. Ulrich, M. Bruns, V. Trouillet, W. Pfleging, Patterning and annealing of nanocrystalline LiCoO2 thin films, J. Optoelectron. Adv. Mater. 12 (3) (2010) 547–552.
[12] R.C. Agrawal, G.P. Pandey, Solid polymer electrolytes: materials designing and all-solid-state battery applications: an overview, J. Phys. D Appl. Phys. 41 (22) (2008) 223001.
[13] B. Huang, C.C. Cook, S. Mui, P.P. Soo, D.H. Staelin, A.M. Mayes, D.R. Sadoway, High energy density, thin-film, rechargeable lithium batteries for marine field operations, J. Power sources 97 (2001) 674–676.
[14] Y.S. Park, S.H. Lee, B.I. Lee, S.K. Joo, All-solid-state lithium thin-film rechargeable battery with lithium manganese oxide, Electrochem. Solid-State Lett. 2 (2) (1999) 58–59.
[15] M. Green, E. Fielder, B. Scrosati, M. Wachtler, J.S. Moreno, Structured silicon anodes for lithium battery applications, Electrochem. Solid-State Lett. 6 (5) (2003) A75–A79.
[16] D. Fujimoto, N. Kuwata, Y. Matsuda, J. Kawamura, F. Kang, Fabrication of solid-state thin-film batteries using LiMnPO 4 thin films deposited by pulsed laser deposition, Thin Solid Films 579 (2015) 81–88.
[17] M. Zhao, Electrochemical Studies of Lithium-ion Battery Anode Materials in Lithium-ion Battery Electrolytes, Doctoral dissertation, Ohio University, 2001.
[18] W.C. West, J.F. Whitacre, B.V. Ratnakumar, Radio frequency magnetron-sputtered LiCoPO4 cathodes for 4.8 V thin-film batteries, J. Electrochem. Soc. 150 (12) (2003). A1660–A16.
[19] H. Xia, L. Lu, G. Ceder, Li diffusion in LiCoO 2 thin films prepared by pulsed laser deposition, J. Power Sources 159 (2) (2006) 1422–1427.
[20] S. Larfaillou, D. Guy-Bouyssou, F. Le Cras, S. Franger, Comprehensive characterization of all-solid-state thin films commercial microbatteries by electrochemical impedance spectroscopy, J. Power Sources 319 (2016) 139–146.
[21] EFL700A39 EnFilm TM Datasheet. www.st.com/enfilm-nb, 2014.
[22] N.H. Kwon, H. Yin, T. Vavrova, J.H. Lim, U. Steiner, B. Grobéty, K.M. Fromm, Nanoparticle shapes of LiMnPO 4, Li+ diffusion orientation and diffusion coefficients for high volumetric energy Li+ ion cathodes, J. Power Sources 342 (2017) 231–240.
[23] N. Nitta, F. Wu, J.T. Lee, G. Yushin, Li-ion battery materials: present and future, Mater. today 18 (5) (2015) 252–264.
[24] M.S. Islam, C.A. Fisher, Lithium and sodium battery cathode materials: computational insights into voltage, diffusion and nanostructural properties, Chem. Soc. Rev. 43 (1) (2014) 185–204.
[25] G.K. Kiran, T.R. Penki, P.V. Kamath, N. Munichandraiah, Effect of orientation on the reversible discharge capacity of electrodeposited Cu2O coatings as lithium-ion battery anodes, J. Solid State Electrochem. 20 (2) (2016) 555–562.
[26] N. Karaman, M. Aliefendić, S. Pljuco, D. Kozlica, N. Nalić, F. Korać, S. Gutić, Solid state synthesis and characterization of LiFePO4/C as cathode material for Li-ion batteries, Bull. Chem. Technol. Bosnia Herzegovina 45 (2015) 19–22.
[27] Y.W. Denis, C. Fietzek, W. Weydanz, K. Donoue, T. Inoue, H. Kurokawa, S. Fujitani, Study of LiFePO4 by cyclic voltammetry, J. Electrochem. Soc. 154 (4) (2007) A253–A257.
[28] W.L. Wang, E.M. Jin, H.B. Gu, Electrochemical performance of lithium iron phosphate by adding graphite nanofiber for lithium ion batteries, Trans. Electr. Electron. Mater. 13 (3) (2012) 121–124.